Microchemical Journal 210 (2025) 113014

Contents lists available at ScienceDirect

Microchemical Journal

journal homepage: www.elsevier.com/locate/microc

# A near-infrared fluorescence probe for selective detection of butyrylcholinesterase and its application in colitis and colorectal cancer diagnosis and therapeutic evaluation

Mo Ma [a,c], Siqi Zhang [a], Jingkang Li [a], Lanyun Zhang [a], Hang Li [b], Xiangqun Jin [c], Pinyi Ma [a,*], Daqian Song [a,*]

[a] College of Chemistry, Jilin Province Research Center for Engineering and Technology of Spectral Analytical Instruments, Jilin University, Qianjin Street 2699, Changchun 130012 China
[b] Department of Hepatobiliary Pancreatic Surgery, China-Japan Union Hospital of Jilin University, Changchun 130033 China
[c] School of Pharmacy, Jilin University, Qianjin Street 2699, Changchun 130012 China

ARTICLE INFO

*Keywords:*
Fluorescence probe
Colitis
Butyrylcholinesterase
Nile Red
Therapeutic evaluation

ABSTRACT

Colitis is a known risk factor for the development and progression of colorectal cancer. Excessive inflammation is a key feature of inflammatory bowel disease (IBD), which is closely linked to colorectal cancer onset. Early and accurate diagnosis of colitis and colorectal cancer is therefore essential for effective intervention. This study presents a novel fluorescence probe, NR-BChE, for the detection of butyrylcholinesterase (BChE) activity. NR-BChE is composed of a hydroxyl Nile Red fluorophore and a BChE-recognition group, cyclopropyl formyl chloride. The probe functions through an intramolecular charge transfer (ICT) mechanism. Upon hydrolysis by BChE, a strong electron donor hydroxyl group is released, the ICT is enhanced and the fluorescence intensity is increased, leading to the emission of red light ($\lambda_{em}$ = 690 nm). The probe has several advantageous properties, including a large Stokes shift (110 nm), low detection limit (0.024 U/L), high selectivity and sensitivity, and excellent biocompatibility. Cellular imaging demonstrated that NR-BChE could effectively detect the elevated BChE levels in colorectal cancer and colitis cells. *In vivo* imaging further revealed that NR-BChE could differentiate normal mouse model from colitis and colorectal cancer mouse models, and evaluate the therapeutic efficacy of four colitis treatment methods. NR-BChE is a new molecular tool for the early diagnosis of colitis and colorectal cancer. It has high potential in the monitoring of disease progression and the evaluation of therapeutic outcomes in clinical settings.

## 1. Introduction

Colitis is a disease characterized by intestinal inflammation, manifesting as damage to the intestinal mucosa and infiltration of inflammatory cells [1]. Chronic colitis can lead to persistent tissue damage and abnormal proliferation of ulcerated intestinal surfaces, which significantly increases the risk of intestinal polyps and colorectal cancer [2–4]. The progression and complications of colitis necessitate early diagnosis and precise monitoring methods to guide effective therapeutic interventions [5]. Colon cancer, a prevalent malignancy of the digestive tract, poses serious health risks. Patients often experience symptoms such as intestinal dysfunction, abdominal pain, diarrhea, constipation, and hematochezia. In addition, cancer cells may disseminate via the blood or lymphatic system to distant organs, including the liver, lungs, and bones, resulting in metastatic lesions that complicate treatment strategies [6–8]. However, traditional diagnostic methods, such as endoscopy and biopsy, are invasive, time-consuming, and unable to provide real-time insights into the dynamic processes of disease progression [9,10]. These limitations highlight the need for non-invasive, sensitive, and specific diagnostic tools, while fluorescence probe technology is a promising alternative that can meet these needs.

Fluorescence probe technology is widely recognized for its high sensitivity, selectivity, and real-time imaging capabilities [11–15]. Its application in inflammatory diseases such as colitis has opened new avenues for disease diagnosis, therapeutic monitoring, and evaluation of treatment efficacy. Researchers can utilize fluorescence probes that can

* Corresponding authors.
*E-mail addresses:* mapinyi@jlu.edu.cn (P. Ma), songdq@jlu.edu.cn (D. Song).

https://doi.org/10.1016/j.microc.2025.113014
Received 4 January 2025; Received in revised form 4 February 2025; Accepted 9 February 2025
Available online 10 February 2025

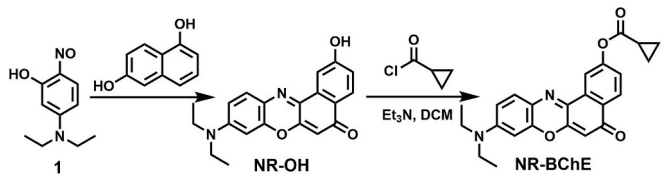


**Fig. 1.** The synthesis process of NR-OH and NR-BChE.

specifically bind to inflam Synthesis of NR-OH:matory biomarkers for real-time imaging and quantitative analysis of inflammatory activity *in vivo* [16–20]. Such probes also enable precise tracking of drug delivery and release to provide insights into the pharmacodynamics of therapeutic agents [21,22]. Emerging research has identified butyrylcholinesterase (BChE) as a potential biomarker of colitis, given its role in modulating inflammation through the cholinergic signaling pathway [23–27]. This discovery not only advances our understanding of colitis pathology but also provides a novel target for diagnostic and therapeutic applications.

Despite these advancements, the design and application of fluorescence probes for colitis remain a bottleneck. Improving the sensitivity and selectivity of these probes is crucial for their broader adoption and clinical utilization [28]. To address these challenges, we synthesized a novel near-infrared fluorescence probe, NR-BChE, using the high quantum yield dye NR-OH as the fluorophore and BChE as the target. The probe emitted light in the near-infrared region (690 nm), which is a spectral range suitable for *in vivo* imaging due to its deep tissue penetration and low background autofluorescence [29]. NR-BChE had high sensitivity and selectivity for BChE and superior lipid droplet-targeting capabilities due to its NR-OH-based structure. Increasing evidence indicates that lipid droplets, organelles in lipid storage and metabolism, are critical players in inflammation [30–32]. With its lipid droplet-targeting ability, NR-BChE could precisely detect inflammatory processes in the intestinal environment. In addition to its diagnostic potential, NR-BChE could be employed to monitor therapeutic responses. The probe could measure both exogenous and endogenous BChE, allowing for a comprehensive evaluation of inflammation dynamics and drug efficacy in colitis mouse models. With its ability to provide real-time visualization of BChE activity, NR-BChE facilitates a better understanding of the interplay between therapeutic agents and inflammatory pathways. NR-BChE is a versatile tool for advancing both basic research and clinical management of colitis.

## 2. Experimental procedure

### 2.1. Organic synthesis

The synthesis process of NR-OH and NR-BChE is illustrated in Fig. 1.

**Synthesis of NR-OH:** Compound 1 was synthesized using a previously reported method [33]. Compound 1 (330 mg, 2 mmol) and 2,6-dihydroxynaphthalene (385 mg, 2.4 mmol) were dissolved in 3 mL of DMF. The reaction mixture was stirred at 150 °C overnight under an inert gas atmosphere. Upon completion, the reaction was cooled to room temperature. Subsequently, 50 mL of saturated saltwater was added to the reaction, followed by ethyl acetate to extract the organic layer. The organic phase was separated, dried with anhydrous sodium sulfate, and concentrated under reduced pressure. The crude product was further purified by silica gel column chromatography using petroleum ether: ethyl acetate (3:1) as the eluent. The purified product NR-OH (a dark red solid) was obtained with a 30 % yield. $^{1}$H NMR (600 MHz, DMSO-$d_6$) $\delta$ 8.21 – 8.13 (m, 2H), 7.61 (d, $J$ = 9.1 Hz, 1H), 7.47 (dd, $J$ = 8.5, 2.4 Hz, 1H), 6.84 (dd, $J$ = 9.1, 2.7 Hz, 1H), 6.66 (d, $J$ = 2.7 Hz, 1H), 6.27 (s, 1H), 3.53 – 3.47 (m, 4H), 1.17 (t, $J$ = 7.1 Hz, 6H) (Fig. S1). $^{13}$C NMR (151 MHz, $CDCl_3$) $\delta$ 182.02, 161.07, 152.07, 151.14, 146.88, 139.18, 134.21, 131.28, 127.93, 124.32, 124.1, 118.82, 110.35, 108.56, 104.55, 96.51, 44.88, 12.91 (Fig. S2). HR-MS ($m/z$): Calculated for $[C_{20}H_{19}N_2O_3]^+$: 335.1390, found: 335.1386 (Fig. S3).

**Synthesis of NR-BChE:** NR-OH (100 mg, 0.3 mmol) was dissolved in anhydrous acetonitrile in a reaction vessel. The solution was placed in an ice bath, and after triethylamine (100 μL, 0.7 mmol) of was added, the mixture was continuously stirred for 5 min. After that, cyclopropyl formyl chloride (100 μL, 1.0 mmol) was added dropwise to the reaction

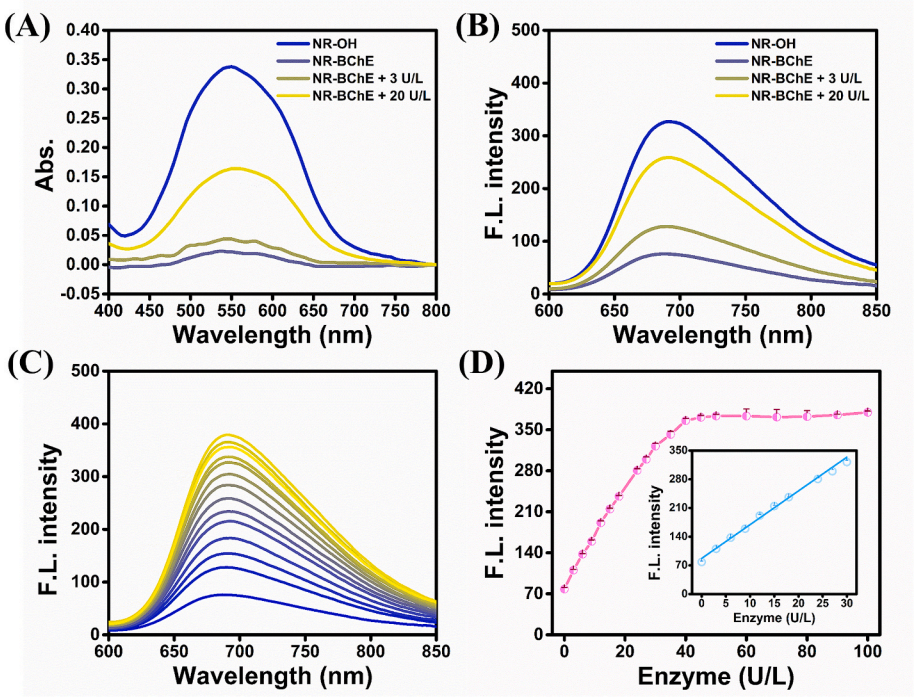


**Fig. 2.** (A) UV–Vis absorption spectra of NR-BChE (10 μM), the reaction system, and NR-OH (10 μM). (B) Fluorescence spectra of NR-BChE (10 μM), the reaction system, and NR-OH (10 μM). (C) Fluorescence spectra of NR-BChE (10 μM) in the presence of BChE at various concentrations. (D) Linear relationship between fluorescence intensity at 690 nm and BChE concentration (0–30 U/L). ($\lambda_{ex}$ = 580 nm).

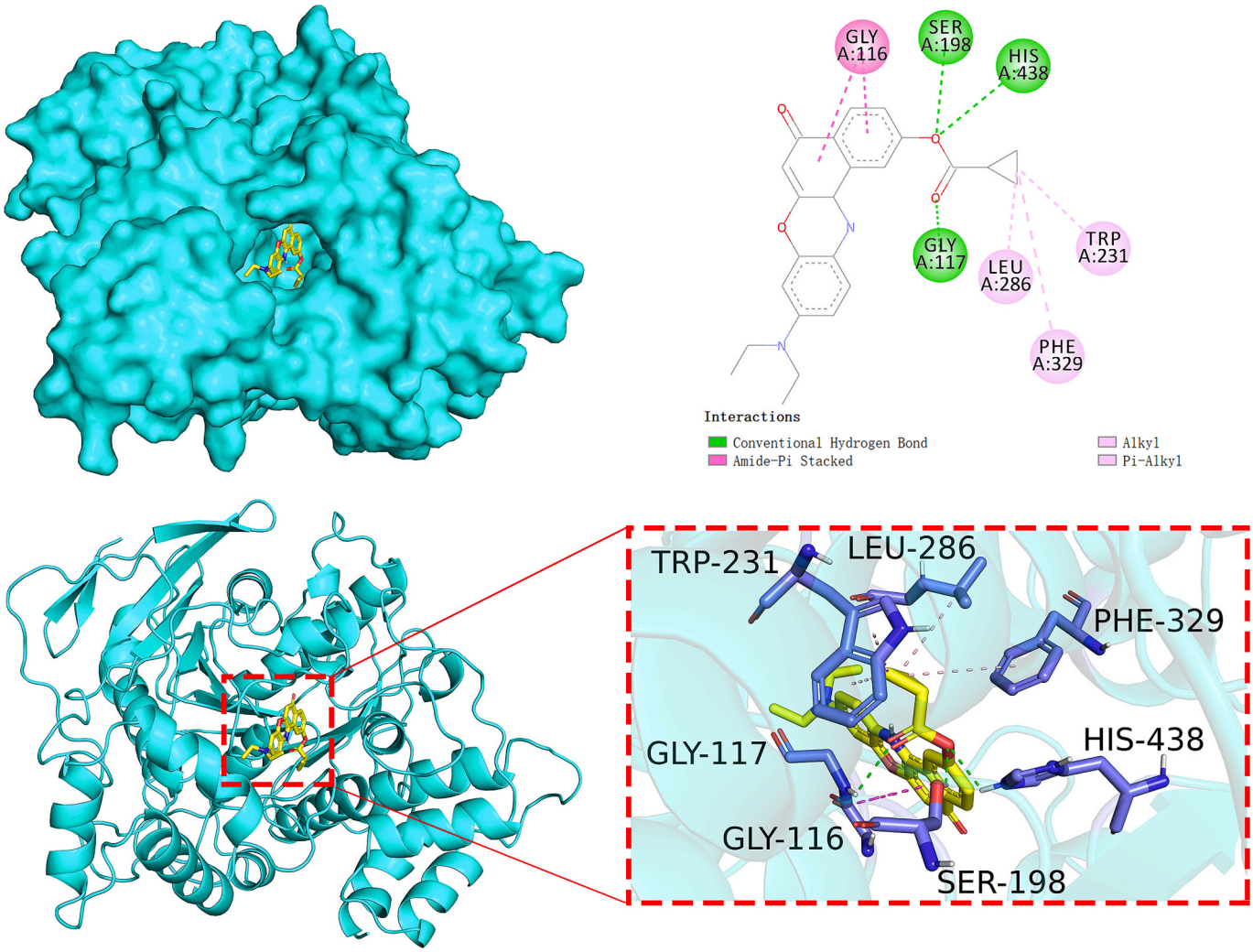


**Fig. 3.** Molecular docking simulation results showing interactions between NR-BChE and BChE.

mixture. After the addition was complete, the mixture was left to stand until the temperature reached room temperature. After that, it was continuously stirred for an additional hour. Once the reaction was complete, the solvent was remo ved under reduced pressure to concentrate the mixture. The crude product was further purified by silica gel column chromatography using petroleum ether:ethyl acetate (3:1) as the eluent. The purified compound NR-BChE (a purple solid) was obtained with a 56 % yield. $^{1}$H NMR (600 MHz, DMSO-$d_6$) $\delta$ 8.21 – 8.13 (m, 2H), 7.61 (d, $J$ = 9.1 Hz, 1H), 7.47 (dd, $J$ = 8.5, 2.4 Hz, 1H), 6.84 (dd, $J$ = 9.1, 2.7 Hz, 1H), 6.66 (d, $J$ = 2.7 Hz, 1H), 6.27 (s, 1H), 3.52 – 3.49 (m, 4H), 2.00 – 1.96 (m, 1H), 1.17 (t, $J$ = 7.1 Hz, 6H), 0.60 (m, 2H), 0.47 (m, 2H) (Fig. S4). $^{13}$C NMR (151 MHz, $CDCl_3$) $\delta$ 181.5, 173.18, 153.31, 152.6, 151.57, 147.07, 137.87, 133.56, 131.55, 129.20, 127.51, 124.72, 124.17, 116.27, 110.93, 104.76, 96.46, 44.98, 12.92, 9.73, 6.56 (Fig. S5). HR-MS ($m/z$): Calculated for $[C_{24}H_{23}N_2O_4]^+$: 403.1652, found: 403.1650 (Fig. S6).

### 2.2. Preparation of samples for spectrophotometric analysis

A stock solution of NR-BChE (1 mM in DMSO) was prepared and stored in a light-protected environment at −40 °C. BChE was dissolved in sterilized water to a final concentration of 50 μg/mL and stored at −80 °C for future use. For spectrophotometric analysis, the NR-BChE stock solution was further diluted in phosphate-buffered saline (PBS, pH 7.4, 10 mM). Appropriate volumes of the BChE solution were added to the NR-BChE solution to achieve the desired final concentrations. The total volume of PBS, NR-BChE, and BChE in each sample was maintained at 300 μL. A control group was prepared under the same conditions without the addition of BChE. All samples, including the control, were incubated on a shaker at 37 °C for 2 h. After incubation, fluorescence emission spectra and UV–visible absorption spectra of the samples were recorded at 37 °C using a 1-cm quartz cuvette, and the data were used for subsequent *in vitro* assays.

### 2.3. Cell imaging

**Fluorescence imaging of NCM460 and SW620 cells:** NCM460 and SW620 cells were incubated with the probe NR-BChE for various durations, and changes in fluorescence signal were observed over time. Fluorescence imaging was performed at different time points, and the dynamic variations of fluorescence signals were evaluated.

**Co-localization experiment:** A co-staining experiment was conducted to confirm the subcellular localization of NR-BChE. SW620 cells were co-incubated with NR-BChE (20 μM) and the commercial dye BODIPY (20 nM) for 90 min. Fluorescence imaging was performed, and the overlap between the probe and the lipid droplet-targeting dye was observed.

**Detection of BChE in inflammatory cells:** The LPS-induced inflammatory response was assessed by treating NCM460 cells with lipopolysaccharide (LPS, 1 μg/mL) for 1 h to induce an inflammatory state, followed by incubating with NR-BChE (10 μM) for 90 min before fluorescence imaging. For Iso-OMPA treatment, NCM460 cells were

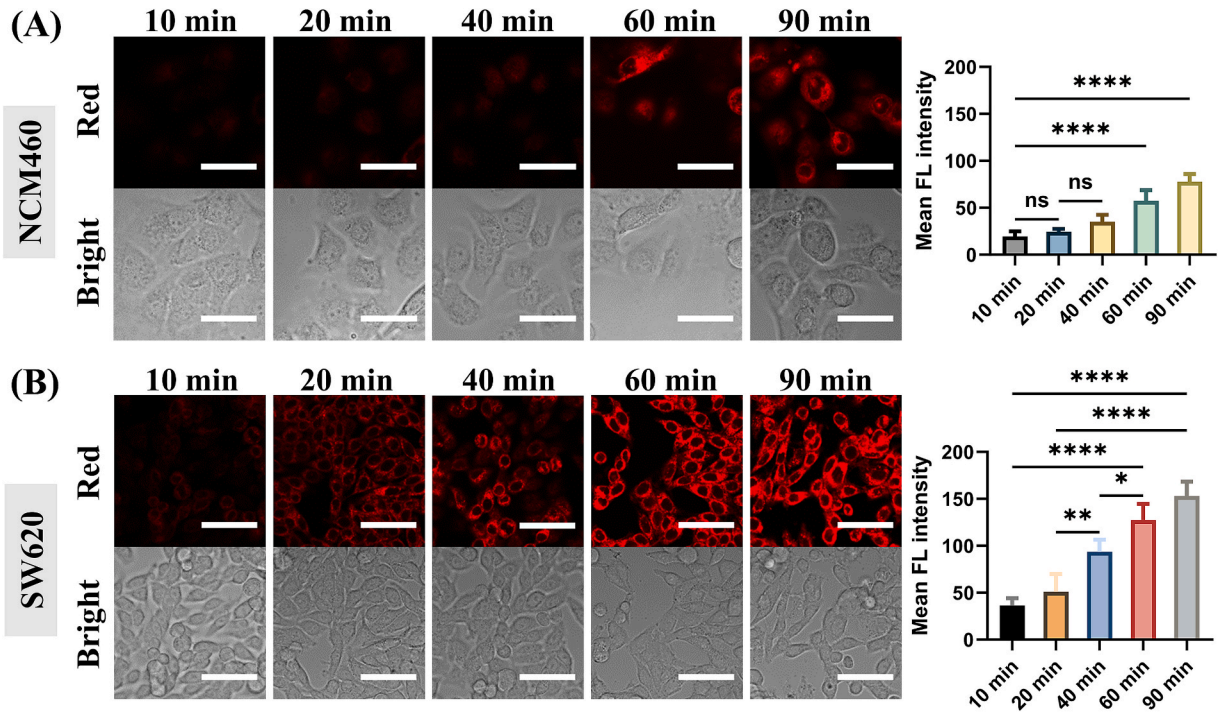


**Fig. 4.** Fluorescence images of NR-BChE (10 μM) in NCM460 cells (A) and SW620 cells (B) captured at different time periods (Left) and the corresponding mean intracellular fluorescence intensity (Right).

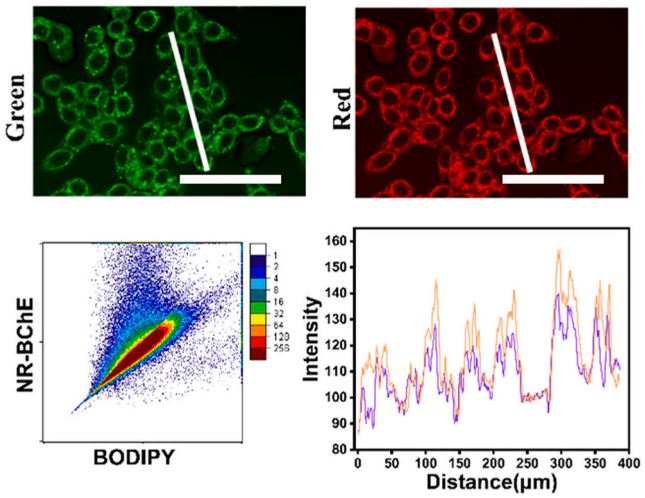


**Fig. 5.** Co-localization of NR-BChE and BODIPY with lipid droplets.

pretreated with *iso*-OMPA (1 mM), a BChE inhibitor, for 1 h, followed by incubation with NR-BChE (10 μM) for 90 min before fluorescence imaging. For hydrocortisone treatment, NCM460 cells were treated with hydrocortisone (1 mM) for 1 h, followed by incubation with NR-BChE (10 μM) for 90 min before fluorescence imaging.

### 2.4. *In vivo imaging of colitis and colon cancer mouse models*

All animal experiments were conducted in compliance with the ethical guidelines approved by Institutional Animal Care and Use Committee (IACUC) of Jilin University, under ethical permit number SY202409006.

**Establishment of colitis mouse model:** A colitis model was established by administering nude mice with 5 % dextran sulfate sodium (DSS) through drinking water for 7 consecutive days. The successful development of colitis was monitored through weight loss and bloody stools.

**Establishment of tumor-bearing mouse model:** Five-week-old specific pathogen-free (SPF) nude mice were housed individually in ventilated cages and fed with standard SPF-grade laboratory chow and water. A suspension of SW620 cells ($2 \times 10^7$ cells in culture medium) was subcutaneously injected into the mice to establish xenograft tumors. The tumors were allowed to grow until their volume reached approximately 200 $mm^3$.

**Treatment groups:** To evaluate therapeutic responses, mice were divided into various treatment groups, and each was administered with the following drugs daily for one week: mesalazine, cyclosporine, BuPiYiChang pills, and FuFang XianHeCao Changyan Pian. Each drug was administered at a volume of 100 μL (16 mM) via oral gavage.

## 3. Results and discussion

### 3.1. *Probe design and spectral performance*

A near-infrared fluorescent probe, NR-BChE, was designed and synthesized. The probe consisted of two key components: the fluorophore (NR-OH) and the BChE-recognition group (cyclopropyl formyl chloride) [25,26,34]. The NR-OH fluorophore emits strong fluorescence, whereas NR-BChE exhibits weak fluorescence due to suppression of the intramolecular charge transfer (ICT) process [35,36]. This suppression arises from the conjugation of cyclopropyl formyl chloride to the hydroxyl group of the fluorophore, which reduces its electron donor capacity. Upon binding to BChE, the probe undergoes enzymatic cleavage, releasing the fluorescent NR-OH.

To study the spectral properties of the probe, the changes in its UV–Vis absorption spectra before and after reacting with BChE at varying amounts were examined. As shown in Fig. 2A, in the absence of BChE, the absorption peak at 580 nm of the probe was negligible. After the addition of BChE, the absorption intensity of the peak at 580 nm increased significantly, and the intensity increased proportionally with enzyme concentration. The peak at 580 nm indicates the formation of

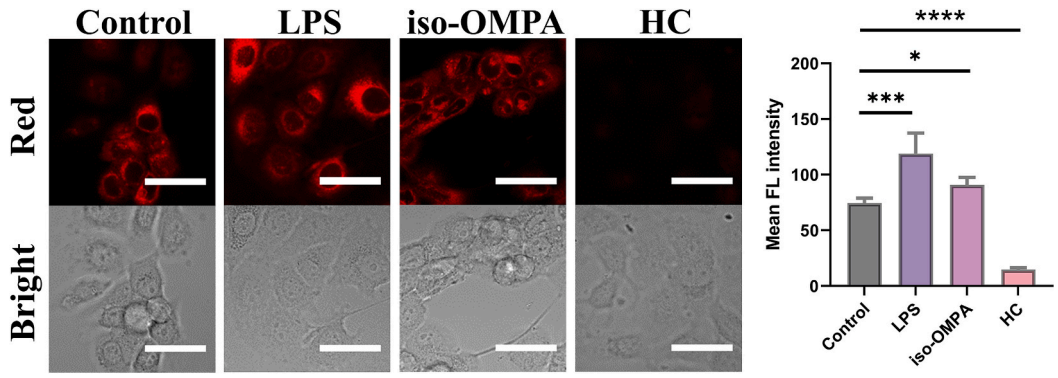


**Fig. 6.** Fluorescence images of NCM460 cells treated with LPS (1 μg/mL), *iso*-OMPA (1 mM), or HC (1 mM) for 1 h, followed by NR-BChE (10 μM) for 90 min (Left) and the corresponding mean intracellular fluorescence intensity (Right).

NR-OH during the enzymatic reaction. The fluorescence spectra of the probe before and after reacting with BChE were analyzed. At an excitation wavelength of 580 nm, the fluorescence intensity at 690 nm markedly increased after the reaction (Fig. 2B). This confirms that a substantial amount of the fluorescent group was formed after the probe reacted with the enzyme.

Further investigation into the fluorescence intensity at 690 nm was conducted by introducing BChE (0–100 U/L) at varying concentrations into the reaction system. The fluorescence intensity was observed to increase progressively with the increase in BChE concentrations, reaching the value 4.68 times higher compared to the control (without BChE) at 100 U/L (Fig. 2C). The fluorescence intensity at 690 nm showed a strong linear relationship with BChE at the concentration range of 0–30 U/L, with a correlation coefficient of $R^2 = 0.996$. This demonstrates the probe's ability to accurately quantify BChE via fluorescence detection (Fig. 2D). The detection limit of the probe, calculated based on a 3S/N criterion, was 0.024 U/L. It was lower than the BChE probes in previously reported (Table S1). This shows that the probe has high sensitivity and potential for precise enzymatic analysis [37–41].

To elucidate the interaction mechanism between the fluorescent probe NR-BChE and BChE, molecular docking simulations were performed. As shown in Fig. 3, NR-BChE forms three hydrogen bonds with GLY117, SER198, and HIS438 in BChE, along with several other weak interactions. These interactions indicate a strong binding affinity between the probe and BChE. The low binding energy of –9.4 kcal/mol further confirms the high stability and specificity of the interaction.

### 3.2. Optimization of spectral properties

The optimization of reaction parameters such as time, pH, and temperature is essential to ensuring the reliability and applicability of the probe in biological systems. These factors influence the efficiency of the probe-enzyme interaction and fluorescence response, as well as the compatibility of the probe with physiological conditions.

Reaction time can directly affect the fluorescence signal and determine the real-time monitoring efficiency of the probe. The fluorescence intensity increased gradually over time, reaching its peak value at 80 min. Beyond this point, the fluorescence intensity remained stable, indicating that NR-Bche possesses good stability and is resistant to decomposition under continuous excitation light irradiation (Fig. S7). Thus, we may conclude that 80 min is the optimal reaction time.

pH plays a vital role in maintaining the stability of the probe and the activity of the enzyme. Fluorescence intensity was analyzed at various pH values. Although the fluorescence signal was not the strongest at pH 7.4, we chose this pH because it reflects the physiological pH (Fig. S8). By selecting pH 7.4, we ensure that the probe can function effectively. This pH also mimics the environment of living organisms.

Temperature is another crucial parameter impacting the enzymatic activity and probe stability. The reaction system was carried out at temperatures of 25 °C, 30 °C, 35 °C, 37 °C, 40 °C, and 45 °C. At 37 °C, although the fluorescence intensity was not the highest, it allows adequate probe-enzyme interaction and aligns with the physiological temperature (Fig. S9). Therefore, 37 °C was selected as the optimal reaction temperature.

The ability of a fluorescent probe to selectively detect its target in complex biological environments is critical for ensuring accurate and reliable measurements. In biological systems, the presence of numerous ions, amino acids, and enzymes can interfere with the probe's performance. To assess the specificity of NR-BChE to its target, the response of the probe to 49 common cations, anions, amino acids, and enzymes was evaluated. As shown in Fig. S10, the fluorescence response of the probe to 49 interfering substances was negligible compared to the response to BChE. This indicates that NR-BChE is not influenced by other biological factors and can selectively detect BChE. These findings underscore the high specificity of NR-BChE to BChE, showing that it is a reliable tool for BChE detection in complex biological environments.

### 3.3. Cellular imaging

To understand the relationship between BChE and colorectal cancer cells, we evaluated the impact of the probe on cell viability to ensure its suitability for subsequent experiments. Cytotoxicity of the probe was assessed using the CCK-8 assay. As shown in Figure S, the viability of NCM460 cells incubated with NR-BChE at different concentrations (0, 10, 20, 30, 50, 100 μM) for 24 h exceeded 90 %. This result indicates that even at high concentrations, NR-BChE does not significantly impact cell viability, which is demonstrative of its low cytotoxicity and suitability in subsequent cellular imaging experiments.

The endogenous levels of BChE in different cell lines were examined using NR-BChE. As shown in Fig. 4A, red fluorescence was observed in NCM460 cells incubated with NR-BChE, and the fluorescence intensity increased over time, reaching the maximum value at 90 min. This indicates the presence of endogenous BChE in NCM460 cells and highlights the excellent cell permeability and ability to detect intracellular BChE activity of the probe. Similarly, SW620 cells incubated with NR-BChE exhibited higher fluorescence intensity compared to NCM460 cells (Fig. 4B). This suggests an overexpression of BChE in SW620 cells and demonstrates the NR-BChE probe's capacity to monitor the variations of BChE levels across cell types.

To explore the subcellular localization of the probe, a co-localization experiment was conducted using the lipid droplet-targeting dye BODIPY [42]. Hydroxyl Nile Red, the core structure of NR-BChE, is known for its lipid droplet-targeting capability [43]. As shown in Fig. 5, the red fluorescence of NR-BChE significantly overlapped with the green fluorescence of BODIPY with a Pearson correlation coefficient of 0. 968. This confirms that NR-BChE predominantly localizes in the lipid droplets, which is consistent with the findings reported in the literature [44]. This also demonstrates the potential of this probe as a lipid droplet-targeting

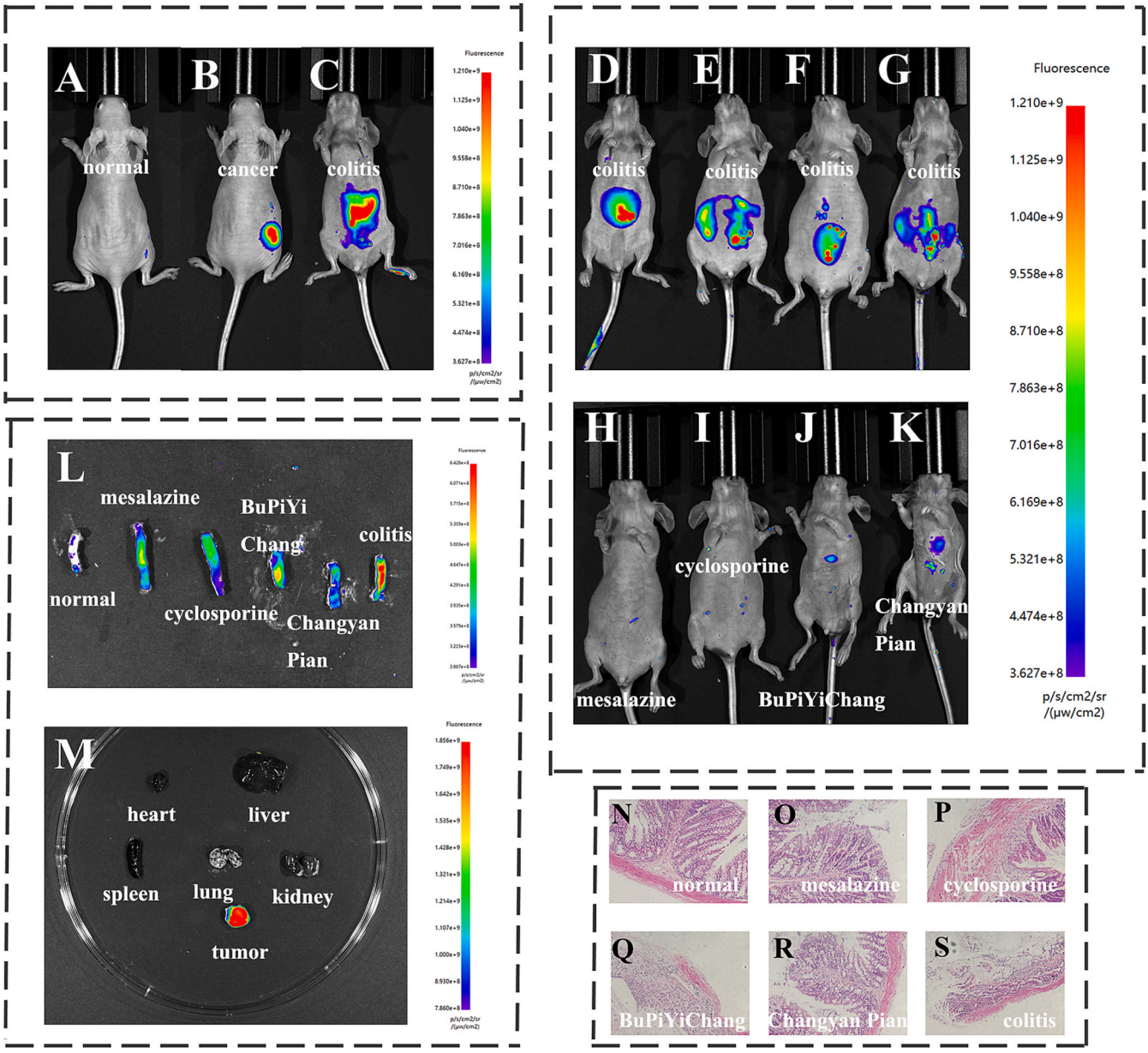


**Fig. 7.** (A-C) Fluorescence images of normal mouse (A), colorectal cancer mouse (B), and colitis mouse (C). (D-G) Fluorescence images of colitis mice. (H-K) Fluorescence images of colitis mice after treatment with four drugs: mesalazine, cyclosporine, BuPiYiChang pills, and FuFang XianHeCao Changyan Pian (from left to right). (L) *Ex vivo* fluorescence images of dissected colons after treatment (from left to right: normal colon, mesalazine-, cyclosporine-, BuPiYiChang pills-, FuFang XianHeCao Changyan Pian-treated colons, colitis). (M) *Ex vivo* fluorescence images of various organs (heart, liver, spleen, lungs, kidneys) and tumor tissue. (N-S) H&E-stained histological images of colons (from left to right: normal colon, mesalazine-, cyclosporine-, BuPiYiChang pills-, FuFang XianHeCao Changyan Pian-treated colons, colitis).

probe for biological applications. NR-BChE is the first probe localized in a lipid drop compared with the BChE probes in previously reported methods (Table S1).

The connection between inflammation and BChE expression was further explored using NCM460 cells. Previous studies have reported a link between inflammation and BChE production [24,45]. As shown in Fig. 6, NCM460 cells treated with LPS, a BChE inducer, had the highest fluorescence intensity, which is an indication of increased BChE activity under inflammatory conditions. Treatment with the BChE activator *iso*-OMPA resulted in a moderate increase in fluorescence intensity; however, the increase was less pronounced compared to LPS. Conversely, the treatment with hydrocortisone (HC), a BChE inhibitor, led to a significant decrease in fluorescence intensity, which reflects the reduction of BChE activity. These results confirm that NR-BChE is highly sensitive to changes in intracellular BChE activity, indicating that it can effectively monitor the dynamic fluctuations in BChE levels.

In summary, NR-BChE can detect endogenous BChE activity, co-localize with lipid droplets, and monitor BChE activity under inflammatory conditions. These findings show that NR-BChE is a powerful tool for studying BChE-related activities and dynamics in biological systems.

### 3.4. *In vivo imaging and therapeutic evaluation*

Previous experiments demonstrated that the NR-BChE probe had excellent spectral properties and was effective in detecting cellular BChE. To extend its application to *in vivo* studies, the biocompatibility of the probe was first assessed using hemolysis tests. As shown in Fig. S12, the probe exhibited a low hemolysis rate, confirming its suitability for *in*

*vivo* imaging applications. Following this, mouse models were constructed to investigate the probe's *in vivo* performance. During the induction of colitis using DSS, a gradual decline in mouse body weight was observed, confirming the successful establishment of the colitis model (Fig. S13B). Fluorescence imaging of normal, colitis, and cancer-bearing mice was conducted (Fig. 7A-C). The results revealed slightly elevated fluorescence intensity in cancer-bearing mice, with clear localization of fluorescence in the dissected tumor tissues compared to other organs (heart, liver, spleen, lungs, and kidneys) (Fig. 7M). The fluorescence intensity of colitis mice was, however, significantly higher than that of normal and cancer-bearing mice, an indication of an abnormally elevated BChE expression level in colitis.

Given their high BChE expression, colitis mice was used in the investigation of the therapeutic effects of different drugs. Four treatment groups of mice were established, and each was administered with the following drugs: mesalazine, cyclosporine, BuPiYiChang pills, and FuFang XianHeCao Changyan Pian. As shown in Fig. S13, the treatment led to a gradual improvement of colitis conditions, as reflected by the partial recovery of body weight. To assess its effectiveness in monitoring the treatment, the NR-BChE probe was injected into the mice, and fluorescence imaging was performed. The results (Fig. 7D-K) demonstrated a decrease in fluorescence intensity during the treatment, indicating a reduction in BChE levels. Among all treatment groups, mesalazine had the highest therapeutic effect, as reflected by its lowest fluorescence intensity. Colon tissues from normal, colitis, and treated mice were extracted and subjected to *ex vivo* fluorescence analysis (Fig. 7L). The fluorescence intensity of normal mice was negligible. Additionally, the fluorescence intensity of treated mice was lower compared to that of untreated colitis mice, which is consistent with the *in vivo* imaging results. These findings further corroborate the efficacy of the therapeutic agents in ameliorating colitis. Histological analysis was conducted to validate the successful establishment of the mouse models and assess the therapeutic effects. As shown in Fig. 7N-S, colon tissue sections from normal mice had normal morphology, while those from colitis mice exhibited significant pathological changes. After drug treatment, the pathological state of the colon tissue of colitis mice gradually improved, approaching normal morphology. These histological results align with the observed body weight recovery, confirming the effectiveness of the four drugs in treating colitis.

These findings demonstrate that the NR-BChE probe can effectively monitor the BChE expression levels in colitis and colorectal cancer mouse models. The probe is suitable as a novel tool for evaluating the therapeutic efficacy of colitis treatments. These results highlight the potential of NR-BChE for *in vivo* studies of BChE-related diseases and their treatments.

## 4. Conclusions

We successfully designed and developed an organic small-molecule fluorescent probe, NR-BChE, for the selective detection of BChE activity. The probe could be recognized by BChE and trigger the release of the fluorophore NR-OH, which caused the enhancement of ICT, leading to the emission of red fluorescence ($\lambda_{em}$ = 690 nm). NR-BChE had a large Stokes shift (110 nm), and high selectivity, sensitivity, and biocompatibility; thus, it is suitable for biological applications. Cellular imaging experiments using the probe revealed elevated BChE expression levels in colorectal cancer cells compared to normal cells. The probe could effectively distinguish colorectal cancer cells from normal cells by selectively labeling endogenous BChE and targeting lipid droplets in the cells. These results underscore the potential of the NR-BChE probe as a tool for differentiating between diseases at the cellular level. *In vivo* imaging studies demonstrated that NR-BChE could clearly distinguish between colitis and colorectal cancer mouse models. Furthermore, the probe was used to evaluate the therapeutic efficacy of four different drugs commonly used for the treatment of colitis. The results showed that NR-BChE could sensitively monitor changes in BChE activity caused by the treatment, and mesalazine was found to provide the best therapeutic outcome. Overall, NR-BChE can be used as an innovative molecular tool for the early diagnosis of diseases related to colitis and colorectal cancer and the evaluation of drug efficacy. The probe has potential in clinical applications including the diagnosis and therapy of colitis and colorectal cancer.

## CRediT authorship contribution statement

**Mo Ma:** Writing – original draft, Validation, Investigation, Data curation, Conceptualization. **Siqi Zhang:** Software, Investigation, Formal analysis. **Jingkang Li:** Writing – review & editing, Resources, Investigation. **Lanyun Zhang:** Writing – review & editing, Validation. **Hang Li:** Writing – review & editing, Validation. **Xiangqun Jin:** Writing – review & editing, Data curation. **Pinyi Ma:** Writing – review & editing, Project administration, Funding acquisition, Data curation, Conceptualization. **Daqian Song:** Supervision, Resources, Project administration, Funding acquisition.

## Declaration of competing interest

The authors declare that they have no known competing financial interests or personal relationships that could have appeared to influence the work reported in this paper.

## Acknowledgments

This work was supported by the National Natural Science Foundation of China (22004046 and 22074052), the Jilin Provincial Natural Science Foundation (20210101457JC).

## Appendix A. Supplementary data

Supplementary data to this article can be found online at https://doi.org/10.1016/j.microc.2025.113014.

## Data availability

Data will be made available on request.

## References

[1] C. Langner, F. Magro, A. Driessen, A. Ensari, G.J. Mantzaris, V. Villanacci, G. Becheanu, P.B. Nunes, G. Cathomas, W. Fries, A. Jouret-Mourin, C. Mescoli, G. de Petris, C.A. Rubio, N.A. Shepherd, M. Vieth, R. Eliakim, K. Geboes, The histopathological approach to inflammatory bowel disease: a practice guide, Virchows Arch. 464 (2014) 511–527.
[2] G. Rogler, Chronic ulcerative colitis and colorectal cancer, Cancer Lett. 345 (2014) 235–241.
[3] S.C. Shah, S.H. Itzkowitz, Colorectal Cancer in Inflammatory Bowel Disease: Mechanisms and Management, Gastroenterology 162 (2022) 715–730.e713.
[4] S.M.M. Borowitz, The epidemiology of inflammatory bowel disease: Clues to pathogenesis? Front. Pediatr. 10 (2023) 1103713.
[5] N.M. Noor, P. Sousa, S. Paul, X. Roblin, Early Diagnosis, Early Stratification, and Early Intervention to Deliver Precision Medicine in IBD, Inflamm. Bowel Dis. 28 (2022) 1254–1264.
[6] D.H. Patel, S. Dang, F.R. Bentley, R.N. Julka, K.W. Olden, F. Aduli, Carcinosarcoma of the Colon: A Rare Cause of Colovesical Fistula, Am. Surg. 75 (2009) 335–337.
[7] M. Riihimaki, A. Hemminki, J. Sundquist, K. Hemminki, Patterns of metastasis in colon and rectal cancer, Sci. Rep. 6 (2016) 29765.
[8] I. Pacal, D. Karaboga, A. Basturk, B. Akay, U. Nalbantoglu, A comprehensive review of deep learning in colon cancer, Comput. Biol. Med. 126 (2020) 104003.
[9] Y. Zhang, G. Zhang, Z. Zeng, K. Pu, Activatable molecular probes for fluorescence-guided surgery, endoscopy and tissue biopsy, Chem. Soc. Rev. 51 (2022) 566–593.
[10] S.M. Hong, D.H. Baek, Diagnostic procedures for inflammatory bowel disease: laboratory, endoscopy, pathology, imaging, and beyond, Diagnostics 14 (2024) 1384.
[11] X. Wu, R. Wang, N. Kwon, H. Ma, J. Yoon, Activatable fluorescent probes for in situ imaging of enzymes, Chem. Soc. Rev. 51 (2022) 450–463.
[12] H. Fang, Y. Chen, Z. Jiang, W. He, Z. Guo, Fluorescent Probes for Biological Species and Microenvironments: from Rational Design to Bioimaging Applications, Acc. Chem. Res. 56 (2023) 258–269.

[13] J. Zhan, W. Song, E. Ge, L. Dai, W. Lin, Reversible fluorescent probes for biological dynamic imaging: Current advances and future prospects, Coord. Chem. Rev. 493 (2023) 215321.
[14] K. Hu, Q. Guo, Y. Wu, Y. Lai, Z. Yu, Y. Liao, Z. Zou, K. Huang, Carbon dots@zeolitic imidazolate framework nanoprobe for direct and sensitive butyrylcholinesterase assay with non-enzymatic reaction, Sensors and Actuators B-Chemical 387 (2023) 133825.
[15] Q. Yu, Q. Guo, J. Zhou, X. Yuan, K. Huang, P. Chen, Filter-assisted smartphone colorimetry/ICP-MS dual-mode biosensor of butyrylcholinesterase in clinical samples, Sensors and Actuators B-Chemical 370 (2022).
[16] J. Li, J. Cao, W. Wu, L. Xu, S. Zhang, P. Ma, Q. Wu, D. Song, A molecular imaging tool for monitoring carboxylesterase 2 during early diagnosis of liver-related diseases, Sensors and Actuators B-Chemical 377 (2023) 133122.
[17] S. Zhang, M. Ma, J. Li, L. Xu, P. Ma, H. Han, D. Song, Neutrophil elastase specific fluorescent probe for early diagnosis of thyroiditis via serum sample testing and fluorescence imaging, Sensors and Actuators B-Chemical 423 (2025) 136736.
[18] S. Zhang, M. Ma, J. Li, J. Li, L. Xu, D. Gao, P. Ma, H. Han, D. Song, A Pyroglutamate Aminopeptidase 1 Responsive Fluorescence Imaging Probe for Real-Time Rapid Differentiation between Thyroiditis and Thyroid Cancer, Anal. Chem. 96 (2024) 5897–5905.
[19] C. Li, S. Zhou, J. Chen, X. Jiang, Fluorescence Imaging of Inflammation with Optical Probes, Chemical & Biomedical Imaging 1 (2023) 495–508.
[20] G. Li, L. Zhang, H. Zheng, W. Lin, Photoacoustic probes for inflammation-related biomarker imaging: Mechanisms, design, and applications, Coord. Chem. Rev. 517 (2024) 215975.
[21] M. Gao, F. Yu, C. Lv, J. Choo, L. Chen, Fluorescent chemical probes for accurate tumor diagnosis and targeting therapy, Chem. Soc. Rev. 46 (2017) 2237–2271.
[22] A. Sharma, P. Verwilst, M. Li, D. Ma, N. Singh, J. Yoo, Y. Kim, Y. Yang, J.-H. Zhu, H. Huang, X.-L. Hu, X.-P. He, L. Zeng, T.D. James, X. Peng, J.L. Sessler, J.S. Kim, Theranostic Fluorescent Probes, Chem. Rev. 124 (2024) 2699–2804.
[23] M.P. Dimopoulos, G.I. Verras, F. Mulita, Editorial: Newest challenges and advances in the treatment of colorectal disorders; from predictive biomarkers to minimally invasive techniques, Front. Surg. 11 (2024) 1487878.
[24] L. Santarpia, I. Grandone, F. Contaldo, F. Pasanisi, Butyrylcholinesterase as a prognostic marker: a review of the literature, J. Cachexia. Sarcopenia Muscle 4 (2013) 31–39.
[25] Z. Zhang, J. Li, B. Yang, M. Ma, X. Ding, H. Shi, P. Ma, D. Song, Z. Zhang, Near-infrared fluorescent probe for ultrasensitive detection of organophosphorus pesticides and visualization of their interaction with butyrylcholinesterase in living cells, Talanta 279 (2024) 126587.
[26] J. Ma, X. Lu, H. Zhai, Q. Li, L. Qiao, Y. Guo, Rational design of a near-infrared fluorescence probe for highly selective sensing butyrylcholinesterase (BChE) and its bioimaging applications in living cell, Talanta 219 (2020) 121278.
[27] Q. Yu, J. Liao, F. Xu, X. Yuan, X. Xiong, T. Xiao, H. Yu, K. Huang, Developments of spectroscopic biosensors for cholinesterase and its inhibitors in the last decade: an overview, Appl. Spectrosc. Rev. 58 (2023) 271–295.
[28] S.O. Kelley, C.A. Mirkin, D.R. Walt, R.F. Ismagilov, M. Toner, E.H. Sargent, Advancing the speed, sensitivity and accuracy of biomolecular detection using multi-length-scale engineering, Nat. Nanotechnol. 9 (2014) 969–980.
[29] J.V. Frangioni, In vivo near-infrared fluorescence imaging, Curr. Opin. Chem. Biol. 7 (2003) 626–634.
[30] Y.X. Zhou, S.Y. Wu, X. Zhang, F.G. Wu, Lipid droplet-targeting optical biosensors: Design strategies and applications, Trac-Trends in Analytical Chemistry 175 (2024) 117703.
[31] A. Zadoorian, X. Du, H. Yang, Lipid droplet biogenesis and functions in health and disease, Nature Reviews, Endocrinology 19 (2023) 443–459.
[32] L. Fan, X. Wang, Q. Zan, L. Fan, F. Li, Y. Yang, C. Zhang, S. Shuang, C. Dong, Lipid Droplet-Specific Fluorescent Probe for In Vivo Visualization of Polarity in Fatty Liver, Inflammation, and Cancer Models, Anal. Chem. 93 (2021) 8019–8026.
[33] Q. Diao, H. Guo, Z. Yang, W. Luo, T. Li, D. Hou, Design of a Nile red-based NIR fluorescent probe for the detection of hydrogen peroxide in living cells, Spectrochimica Acta Part a-Molecular and Biomolecular Spectroscopy 223 (2019) 117284.
[34] J. Guo, J. Sun, D. Liu, J. Liu, L. Gui, M. Luo, D. Kong, S. Wusiman, C. Yang, T. Liu, Z. Yuan, R. Li, Developing a Two-Photon "AND" Logic Probe and Its Application in Alzheimer's Disease Differentiation, Anal. Chem. 95 (2023) 16868–16876.
[35] L. Xu, M. Ma, J. Li, H. Yang, D. Gao, P. Ma, D. Song, Exploring butyrylcholinesterase expression in diseases using a promising fluorescent imaging tool, Sens. Actuators B 394 (2023) 134432.
[36] H. Dong, L. Zhao, T. Wang, Y. Chen, W. Hao, Z. Zhang, Y. Hao, C. Zhang, X. Wei, Y. Zhang, Y. Zhou, M. Xu, Dual-Mode Ratiometric Electrochemical and Turn-On Fluorescent Detection of Butyrylcholinesterase Utilizing a Single Probe for the Diagnosis of Alzheimer's Disease, Anal. Chem. 95 (2023) 8340–8347.
[37] Y. Yang, L. Zhang, J. Wang, Y. Cao, W. Qin, Y. Liu, Real-time fluorescent determination and biological imaging in living models via a butyrylcholinesterase-activated fluorescent probe, Dyes Pigm. 206 (2022) 110596.
[38] W. Kang, M. Ma, L. Xu, S. Tang, J. Li, P. Ma, D. Song, Y. Sun, Customized fluorescent probe for peering into the expression of butyrylcholinesterase in thyroid cancer, Anal Chim Acta 1282 (2023) 341932.
[39] S. Yoo, M.S. Han, A fluorescent probe for butyrylcholinesterase activity in human serum based on a fluorophore with specific binding affinity for human serum albumin, Chemical, Communication 55 (2019) 14574–14577.
[40] Q. Zhang, C. Fu, X. Guo, J. Gao, P. Zhang, C. Ding, Fluorescent Determination of Butyrylcholinesterase Activity and Its Application in Biological Imaging and Pesticide Residue Detection, ACS Sensors 6 (2021) 1138–1146.
[41] Z. Yu, X. Li, X. Lu, Y. Guo, Rational construction of a novel probe for the rapid detection of butyrylcholinesterase stress changes in apoptotic cells, New J. Chem. 46 (2022) 12034–12040.
[42] Y. Li, Y. Wang, Y. Li, W. Shi, J. Yan, Construction and evaluation of near-infrared fluorescent probes for imaging lipid droplet and lysosomal viscosity, Spectrochim. Acta Part A-Mol. Biomol. Spectrosc. 316 (2024) 124356.
[43] S. Fukumoto, T. Fujimoto, Deformation of lipid droplets in fixed samples, Histochem. Cell Biol. 118 (2002) 423–428.
[44] H. Huang, Y. Bu, Z.-P. Yu, M. Rong, R. Li, Z. Wang, J. Zhang, X. Zhu, L. Wang, H. Zhou, Solvatochromic Two-Photon Fluorescent Probe Enables In Situ Lipid Droplet Multidynamics Tracking for Nonalcoholic Fatty Liver and Inflammation Diagnoses, Anal. Chem. 94 (2022) 13396–13403.
[45] U.N. Das, Acetylcholinesterase and butyrylcholinesterase as possible markers of low-grade systemic inflammation, Med. Sci. Monit. 13 (2007) RA214-RA221.